Kinetic Characterization of Mass Transfer Limited Biodegradation of a Low Water Soluble Gas in Batch Experiments—Necessity for Multiresponse Fitting

Bart De heyder,[1,3] Peter Vanrolleghem,[2] Herman Van Langenhove,[3] Willy Verstraete[1]

[1]Laboratory of Microbial Ecology, Faculty of Agricultural and Applied Biological Sciences, University of Gent, Coupure Links 653, B-9000 Gent, Belgium; telephone: 32-9-264.59.76; fax: 32-9-264.62.48; e-mail: willy.verstraete@rug.ac.be
[2]Department of Applied Mathematics, Biometrics and Process Control, Faculty of Agricultural and Applied Biological Sciences, University of Gent, Belgium
[3]Department of Organic Chemistry, Faculty of Agricultural and Applied Biological Sciences, University of Gent, Belgium

Received 8 August 1996; accepted 10 January 1997

Abstract: A method was developed to characterize the kinetics of biodegradation of low water soluble gaseous compounds in batch experiments. The degradation of ethene by resting *Mycobacterium* E3 cells was used as a model system. The batch degradation data were recorded as the progress curve (i.e., the time course of the ethene concentration in the headspace of the batch vessel). The recorded progress curves, however, suffered gas:liquid mass transfer limitation. A new multiresponse fitting method had to be developed to allow unequivocal identification of both the affinity coefficient, K_{aff}, and the gas:liquid mass transfer coefficient, K_la, in the batch vessel from the mass transfer limited data. Simulation showed that the K_{aff} estimate obtained is influenced by the dimensionless (volumetric basis) ethene gas:liquid partitioning coefficient (H). In the fitting procedure, Monod, Teissier, and Blackman biokinetics were evaluated for characterization of the ethene biodegradation process. The fits obtained reflected the superiority of the Blackman biokinetic function. Overall, it appears that resting *Mycobacterium* E3 cells metabolizing ethene at 24°C have, using Blackman biokinetics, a maximum specific degradation rate, v_{max}, of 10.2 nmol C_2H_4 mg^{-1} CDW min^{-1}, and an affinity coefficient, $K_{aff,g}$, expressed in equilibrium gas concentration units, of 61.9 ppm, when H is assumed equal to 8.309. *Biotechnol Bioeng* **55**: 511–519, 1997.
Keywords: ethene; kinetics; biodegradation; mass transfer; multiresponse fitting

INTRODUCTION

The kinetic characterization of microbial degradation processes involves several steps: (i) design of the experimental set-up to collect the biodegradation data; (ii) formulation of a biophysical model that describes the experimental set-up and incorporates a biokinetic function describing the relation between the specific biodegradation rate and the concentration of the compound; (iii) selection of a mathematical technique to fit the biophysical model to the collected biodegradation data allowing estimation of the biokinetic parameters of the biokinetic function.

For the design of the experimental set-up, practical factors such as, for instance, the availability of reactor equipment or analytical equipment, play an important role. Especially for gaseous compounds, which are generally more difficult to manipulate than solid or liquid compounds, the simplicity of the experimental set-up is a decisive factor. The characterization procedure for gaseous compounds is therefore, in most cases, based on batch experiments (de Bont, 1976; Robinson and Tiedje, 1982, 1983; van Ginkel and de Bont, 1986; van Ginkel et al., 1986). The batch experimental set-up involves injection of the compound in the headspace of a gas-tight batch vessel containing a microbial suspension. The concentration of the compound in the headspace will decrease as a result of a combined gas:liquid mass transfer and biodegradation process. The decrease of the gas concentration as a function of time, referred to as the progress curve, can easily be collected by regular sampling of the headspace, and represents the biodegradation data used for the fitting of a biophysical model.

The biophysical model should, in principle, consider both the gas:liquid mass transfer and biodegradation process. However, in several cases, it is assumed that the gas:liquid mass transfer rate is sufficiently high so that the course of the progress curve is determined solely by the biodegradation process (de Bont, 1976; Robinson and Tiedje, 1983; van Ginkel and de Bont, 1986; van Ginkel et al., 1986).

Correspondence to: W. Verstraete
Contract grant sponsors: Institute for Promotion of Scientifique Research in Industry and Agriculture; Flemish Impulse Programme for Environmental Technology; Belgian National Fund for Scientific Research

 CCC 0006-3592/97/030511-09

Consequently, if the progress curve is limited by gas:liquid mass transfer, a modeling error will be lumped into erroneous biokinetic parameter estimates. The risk for gas:liquid mass transfer limitation increases as: (i) the biodegradation rate increases (e.g., at higher biomass concentrations); (ii) the gas:liquid mass transfer coefficient decreases (e.g., under less intense mixing conditions); or (iii) the driving force for mass transfer decreases (e.g., at lower gas concentrations). Experimental conditions where gas:liquid mass transfer limitation is absent can thus be met by, for instance, decreasing the biodegradation rate through appropriate dilution of the microbial suspension (de Bont, 1976; Robinson and Tiedje, 1982). Robinson and Tiedje (1982) demonstrated that the estimated biokinetic parameters for H_2 consumption by rumen fluid became constant and independent of the biomass concentration above a critical dilution factor. The determination of the critical dilution factor, however, can require the set-up of many repetitive experiments. Also, when plotting the parameter estimates as a function of the dilution factor, their variability can hamper the evaluation of their constant character above the critical dilution factor.

The biodegradation process incorporated in the biophysical model can be described by different kinds of biokinetic functions. Well-known functions were proposed by Monod, Teissier, and Blackman (Table I). These three functions have in common that they: (i) incorporate two biokinetic parameters (i.e., the maximum specific degradation rate and the affinity coefficient); and (ii) show a saturating behavior (i.e., the specific degradation rate reaches a maximum value at higher compound concentrations). For an identical affinity coefficient, Blackman will saturate first, followed by Teissier and Monod. The different saturation behavior implies that the biokinetic function should be selected carefully. Nevertheless, in most biokinetic studies, the Monod biokinetic function is selected a priori, without consideration of an alternative biokinetic function (Moser, 1985).

This article presents an evaluation of the procedure for kinetic characterization of the microbial degradation of low water soluble gaseous compounds from progress curves recorded in batch experiments using resting cell suspensions. The degradation of ethene by the *Mycobacterium* E3 strain was used as a model system. Special attention was paid to: (i) the selection of the appropriate biokinetic function; (ii) the detection of mass transfer limitation; (iii) the development of a new multiresponse method allowing the estimation of the biokinetic parameters from a restricted number of progress curves recorded under gas:liquid mass transfer limitation; and (iv) the influence of the dimensionless gas:liquid partitioning coefficient on the estimated parameters.

Table I. The Blackman, Teissier, and Monod biokinetic functions.

Function	Corresponding equation
Blackman[a]	$\begin{cases} v = v_{max}\dfrac{C_l}{2K_{aff,l}} & \text{for } C_l < 2K_{aff} \\ v = v_{max} & \text{for } C_1 \geqslant 2K_a \end{cases}$
Teissier[a]	$v = v_{max}\left(1 - \exp\left(-\dfrac{C_l}{K_{aff,l}}\ln(2)\right)\right)$
Monod	$v = v_{max}\dfrac{C_l}{K_{aff,l} + C_l}$

[a]The original notation of the Blackman and Teissier biokinetic functions was transformed so that the affinity parameter corresponds to the compound concentration at which half of the maximum specific degradation rate is reached. This transformation does not alter the basic behavior of these functions and allows a straightforward comparison of the saturation behavior with Monod.

EXPERIMENTAL

Determination of Ethene

Ethene in the gas phase was analyzed by injecting a 100-μL gas sample using a gas-tight syringe (Hamilton 1710 RN) with Chaney adaptor in a Varian Type 3700 chromatograph fitted with a Porapak N (50°C) column and a FID (200°C). Helium was used as the carrier gas (30 ml min^{-1}). Calibration standards were prepared by adding a precise volume of ethene to evacuated flasks sealed with rubber septa. After the injection of ethene, the calibration flasks were pressurized to atmospheric pressure with ambient air. The GC calibration function (i.e., the linear relationship between the peak area and the concentration value) was calculated using a weighted linear regression (WLR) procedure according to Miller (1991). The weight factors for the WLR were calculated using the squared peak area values. Statistical analysis showed that the peak area errors had a normal distribution and a constant relative error above a threshold peak area value of 5000 (data not shown).

Microorganism

The *Mycobacterium* E3 strain has been described by Habets-Crützen et al. (1984), and was kindly provided by Dr. Sybe Hartmans (Wageningen Agricultural University, Wageningen, NL). Microorganisms were grown in batch at 25°C in shaken serum flasks gas-tight sealed with rubber septa using mineral salts medium (de Bont, 1976). The flasks contained 10% ethene in the gas phase as the sole source of carbon and energy.

Preparation of Resting Cell Suspensions

The experiments were performed using resting cell suspensions (i.e., suspensions of microbial cells in a physiological buffer solution) (Habets-Crützen et al., 1984; van Ginkel and de Bont, 1986; van Ginkel et al., 1986). As a consequence, growth effects are eliminated so that the biomass concentration can be held constant at the required diluted level throughout the whole experiment. The need for estimation of additional biodegradation parameters (e.g., the

yield coefficient) is then circumvented. Microorganisms were harvested by centrifugation at 10°C. The obtained pellet was washed with physiological buffer solution at pH 6.8 (8.5 g L^{-1} NaCl, 0.5 g L^{-1} K_2HPO_4, and 0.5 g L^{-1} KH_2PO_4) and resuspended in the same buffer. The biomass concentration of the prepared concentrated resting cell suspension was quantified as cell dry weight (CDW). Determination of the dry weight of the physiological buffer solution allowed to correct for the salt content. The concentrated resting cell suspension was used to prepare different resting cell suspensions by further dilution with physiological buffer solution. The biomass concentration of each prepared resting cell suspension was calculated using the corresponding dilution factor. The prepared resting cell suspensions were used immediately for simultaneous recording of progress curves.

Recording of Progress Curves

The progress curves were recorded in batch vessels of 118-mL total volume and gas-tight sealed with rubber septa. The volume of the resting cell suspension was 18 mL, the injected volume of ethene was 300 μL. The batch vessels were shaken using a table stirrer (Edmund Bühler SWIP KS-10) at 350 rpm. The progress curves were recorded by determination of the ethene concentration in the headspace of the batch vessel at different time intervals. The sampling was started 10 min after the injection of ethene to prevent the recording of initial transient effects. The influence of variations in pressure in the batch vessel—due to ethene injection, sampling, etc.—on the gas chromatographic analysis could be considered negligible.

Figure 1A shows the three simultaneously recorded progress curves, PC1, PC2, and PC3, which are used further to illustrate the approach for estimation of the biokinetic parameters. Each progress curve corresponds to a different biomass concentration and is characterized by a linear and a nonlinear range, at higher and lower gas concentrations, respectively. The ethene gas concentration intervals over which the progress curves were recorded were approximately equal. Evidently, the time interval of recording was shorter as the biomass concentration was higher. This shorter time interval effected the collection of fewer data points.

BIOPHYSICAL MODELS

The basic set of equations describing both the mass transfer and biodegradation process taking place in the batch vessel is:

$$V_1 \cdot \frac{dC_l}{dt} + V_g \cdot \frac{dC_g}{dt} = - V_l \cdot X \cdot v \qquad (1)$$

$$\frac{dC_g}{dt} = - \frac{V_l}{V_g} \cdot K_l a \cdot (C_l^* - C_l) \qquad (2)$$

$$C_l^* = \frac{C_g}{H} \qquad (3)$$

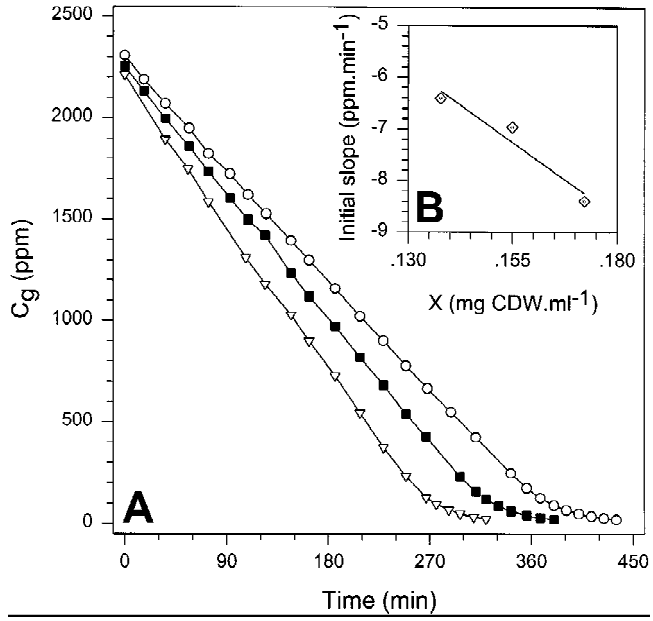

Figure 1. (A) Three progress curves recorded simultaneously at 24°C corresponding to three different biomass concentrations: (○) PCI 26 datapoints, X = 0.1378 mg CDW · mL^{-1}; (■) PC2 23 datapoints, X = 0.1550 mg CDW · mL^{-1}; and (▽) PC3 18 datapoints, X = 0.1722 mg CDW · mL^{-1}. (B) Check for initial mass transfer limitation by evaluation of the proportionality between the initial slope and the biomass concentration. The initial slope of each progress curve was determined by a linear regression using the first five datapoints. The correlation coefficient was, in each case, greater than 0.999.

Eq. (1) represents the mass balance of the compound. The specific degradation rate, v, in this equation must be substituted by one of the biokinetic functions given in Table I. Considering the high intensity of mixing, the limited volume of liquid in the batch vessel, and the limited formation of microbial flocs confirmed by microscopic evaluation, the major resistance for mass transfer is assumed to be located at the gas:liquid interphase. Eqs. (2) and (3) describe the gas:liquid mass transfer of the compound. The set of Eqs. (1), (2), and (3) is subsequently referred to as model I.

In an alternative simplified biophysical model, model II, it is assumed that the course of the progress curve is solely determined by the biodegradation process. The latter assumption implies that the liquid and gaseous compound concentrations are always in equilibrium:

$$C_l = \frac{C_g}{H} \qquad (4)$$

Substitution of Eq. (4) into Eq. (1) allows to obtain the basic equation of model II;

$$\frac{dC_g}{dt} = - \frac{H \cdot V_l}{H \cdot V_g + V_l} \cdot X \cdot v \qquad (5)$$

In model II, the specific degradation rate, v, is expressed as a function of gas concentration, C_g, by substitution of Eq. (4) in the biokinetic functions (Table I). Also, the affinity

parameter, $K_{aff,l}$, is expressed in equilibrium gas concentration units using the relation:

$$K_{aff,g} = H \cdot K_{aff,\,l} \tag{6}$$

The course of a progress curve, as described by model II, will be characterized by a linear range at higher gas concentrations and a nonlinear range at lower gas concentrations (Fig. 2). The biokinetic parameter, v_{max}, influences the linear range. The nonlinear range, on the other hand, is influenced by both the biokinetic parameters, v_{max} and $K_{aff,g}$. Model I will result in the same course as model II if the value of $K_l a$ is sufficiently high (Fig. 2). If not, the gas:liquid mass transfer is limiting, and the nonlinear range of the progress curve is extended to higher concentrations (Fig. 2).

MODEL FITTING

The purpose of model fitting was the estimation of the model parameters such that the model course closely represents experimentally measured variables. The fitting is performed with the aid of an objective function describing the deviation between experiment and model. The estimated parameter values for which the objective function is minimal are accepted as estimates of the true parameter values.

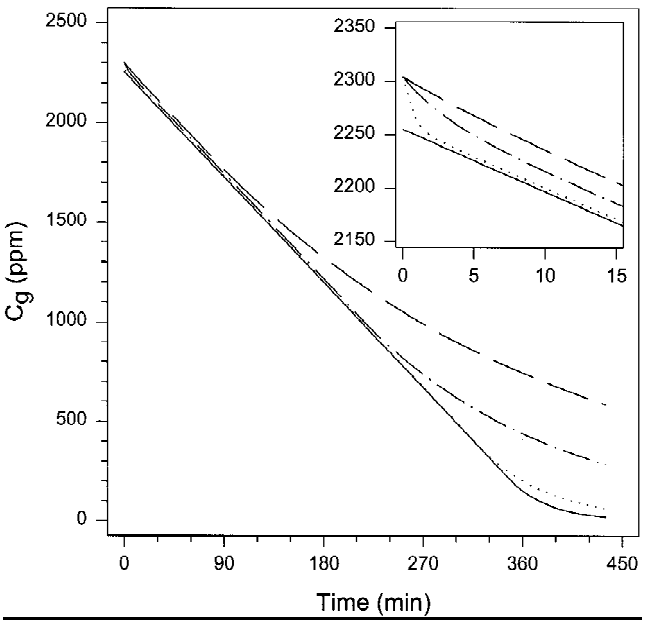

Figure 2. Illustration of the course of a progress curve simulated by model II (—). Influence of mass transfer limitation on the course of a progress curve simulated with model I with implementation of $K_l a$ equal to 10 (- - -), 20 (—•—), and 100 (• • •) h^{-1}. The biokinetic parameters for both models corresponded to v_{max} 9.9 nmd C_2H_4 mg^{-1} CDW min^{-1} and $K_{aff,g}$ 105.5 ppm. All other parameters were in accordance with the experimental set-up. The inset enlarges the initial course of the simulated curves. The initial deviation between biophysical models is caused by the fact that simulation of model I was performed for an initial ethene liquid concentration, C_l, equal to zero.

Considering that the gas chromatographic analysis of ethene is characterized by a constant relative error, the deviation between experiment and model was described by the sum of squared relative residuals (SSR_{rel}) (Robinson, 1985; Saéz and Rittmann, 1992):

$$SSR_{rel} = \sum_{i=1}^{n} \left(\frac{C_{g,est} - C_{g,exp}}{C_{g,exp}} \right)_i^2 \tag{7}$$

where n represents the number of datapoints, and $C_{g,est}$ and $C_{g,exp}$ the estimated and experimental gas concentrations, respectively.

The fitting was performed with the computer program MOSIFIT (Vanrolleghem and Verstraete, 1993). Both model I and model II and the three biokinetic functions (Table I) were implemented. MOSIFIT incorporated a variable step fourth-order Runge–Kutta routine to solve differential equations and used a direction set optimization technique (Brent, 1973) to minimize the objective function. Testing of the fitting procedure showed that the fitting technique featured good convergence properties; that is, the estimated parameter values were independent of the user-specified initial parameter values.

The estimated parameters and variables for model I were compound gas concentration, $C_{g,0}$, and liquid, concentration, $C_{l,0}$, at time zero; the overall gas:liquid mass transfer coefficient, $K_l a$; and the biokinetic parameters, v_{max} and $K_{aff,l}$. The corresponding $K_{aff,g}$ value was calculated according to Eq. (6). The parameters and variables estimated for model II were v_{max}, $K_{aff,g}$, and C_g,0. The corresponding $K_{aff,l}$ value also was calculated using Eq. (6). For both models, the actual values of the estimated compound concentrations at time zero, while being needed for adequate estimation, were of limited interest and are not discussed further. Fixed parameters were the liquid volume, V_l, the gas volume, V_g, the biomass concentration, X, and the dimensionless gas:liquid partitioning coefficient, H. The parameter V_l was equal to the volume of the microbial suspension; V_g was calculated based on the determined volume of the batch vessel and V_l; H corresponded to the reference value for an air:water system at the temperature of the experiment: 8.309 at 24°C (l'Air Liquide, 1976).

Evaluation of the quality of the obtained fit was based mainly on: (i) visual inspection of the fit and distribution of the obtained residuals; (ii) the obtained value of the objective function; and (iii) diagnostic checking of the residuals for their random character with the runs test (Söderström and Stoïca, 1989). The random character of residuals is a basic theoretical assumption when using the SSR_{rel} as objective function (Saéz and Rittmann, 1992).

RESULTS AND DISCUSSION

Checking Mass Transfer Limitation—Fitting Model II

The procedure to detect mass transfer limitation of the recorded progress curves is, as described in what follows, based on evaluation of the biokinetic parameters estimated

by fitting model II. Before that, however, the most appropriate biokinetic function to fit model II had to be selected. Implementation of the three biokinetic functions (Monod, Teissier, and Blackman) in the fitting of model II, showed that the best quality of fit was obtained with the Blackman biokinetic function. The latter is illustrated in detail for progress curve PC1 in Figure 3 and Table II. The sharper saturation behavior of the Blackman biokinetic function results in the ability to accurately follow the relatively sharp transition between the linear and nonlinear range of the recorded progress curves. Also, Moser (1985), suggested that Monod biokinetics can saturate too slowly to be a proper approximation of experimental data. The saturation behavior of the Teissier biokinetic function shows an intermediate behavior. The different saturation behavior of the three biokinetic functions results in different estimated biokinetic parameter values (Table II). A random character of the obtained residuals as evaluated by the runs test, however, could, even with implementation of the Blackman biokinetic function, not always be confirmed. This might indicate that dynamic processes were taking place during the recording of the progress curves which were not incorporated in the biophysical models (e.g., slight temperature variations).

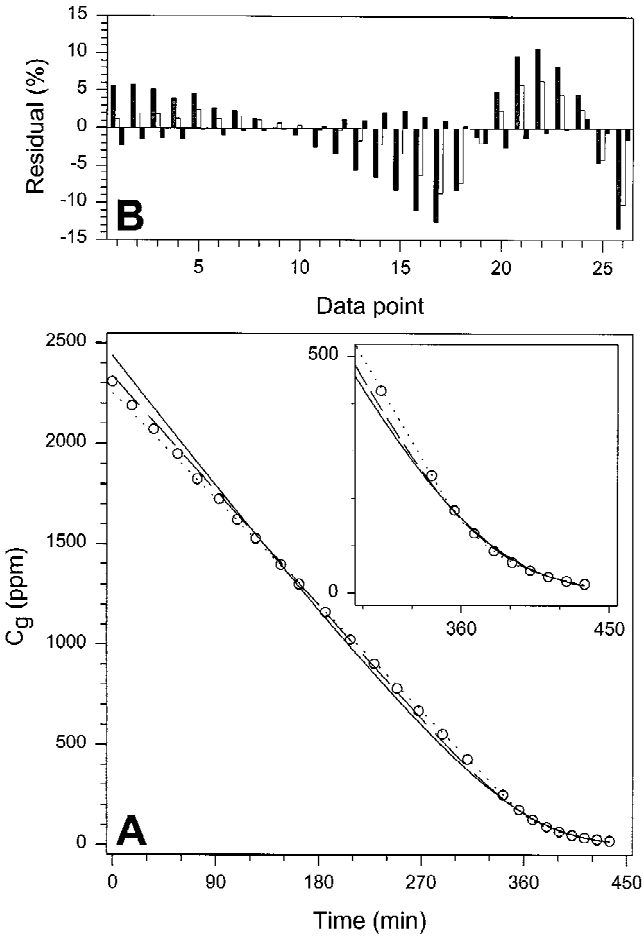

Figure 3. Fitting model II to progress curve PC1. (A) Course of the experimental data (○) and the fitted curves for implementation of the Monod (—), Teissier (- - -), and Blackman (• • •) biokinetic function. (B) The relative residual (%) obtained for each datapoint for implementation of the Monod (▨), Teissier (□), and Blackman (■) biokinetic function.

Table II. Results of fitting Model II to the recorded progress curve PC1 with implementation of the Blackman, Monod, and Teissier biokinetic functions.

Biokinetic function	v_{max} estimate	$K_{aff,g}$ estimate	Minimized SSR_{rel}
Blackman	9.9	105.5	4.37e-03
Teissier	10.7	126.3	4.37e-02
Monod	13.2	198.3	1.18e-01

An overview of the results of fitting Model II to progress curves PC1, PC2, and PC3 with implementation of the Blackman biokinetic function is given in Table III. To detect possible mass transfer limitation, the estimated parameters, v_{max} and $K_{aff,g}$, were used as input for simulation and comparison with model I. This is illustrated for progress curve PC1 in Figure 2. The results showed a clear deviation between model I and model II for in the specified range of K_la, especially in the lower ethene gas concentration range (with nonlinear behavior). For the specified parameter values and the simulated experimental conditions, K_la, values in the order of 2000 h^{-1} are necessary to obtain a deviation between both models less than 10% in the lower gas concentration range. This order of magnitude of K_la, is probably not attainable in shaken batch vessels (Appendix). These simulations, therefore, indicate that the recorded progress curves suffered mass transfer limitation.

The mass transfer limitation, however, does not cause model II to be fit poorly. During the fitting of model II, the model inadequacy is compensated by parameter adjustment; that is, the extended nonlinear range is mathematically interpreted as a higher $K_{aff,g}$ value. The latter results in an overestimation of $K_{aff,g}$, which is a typical symptom of mass transfer limitation (Powel, 1967; Robinson and Tiedje, 1982). Increasing the biomass concentration will cause an initiation of mass transfer limitation at even higher ethene gas concentrations and thus will result in an increasing trend of overestimation of $K_{aff,g}$. The results of fitting model II to the recorded progress curves (Table III) are in accordance with this trend.

The simulation results (Fig. 2) also indicated that mass transfer limitation is not occurring during the initial linear range of the recorded progress curves. This is also indicated

Table III. Results of fitting model II to the progress curves PC1, PC2, and PC3 with implementation of the Blackman biokinetic function.

Progress curve	v_{max} estimate	$K_{aff,g}$ estimate	Minimized SSR_{rel}
PC1	9.9	105.5	4.37e-03
PC2	10.1	111.1	3.40e-03
PC3	10.5	119.6	2.52e-03

by the proportional relationship between the initial slope of the progress curves and the corresponding biomass concentration (Fig. 1B). The absence of mass transfer limitation in the initial linear range of the recorded progress curves should allow estimation of v_{max} by fitting model II. This was confirmed by fitting model II to synthetic progress curves suffering mass transfer limitation in the nonlinear range only, simulated with model I (data not shown). The estimates of v_{max} in Table III are thus acceptable. The observed difference in estimated v_{max} for the three progress curves might be caused by an error in the biomass concentration which has to be specified for fitting the progress curves.

Parameter Identifiability Problem—Fitting Model I

Because the mass transfer process is incorporated in model I, more reliable parameter estimates should be obtained by fitting model I. The fitting of model I, however, requires either the estimation or input of the actual K_la value. No K_la value for ethene transfer in the batch vessel was available so, therefore, this value had to be estimated from the recorded progress curves. Fitting experiments, however, showed that implementing different hypothetical K_la values resulted in different estimates of $K_{aff,g}$ without affecting the fit quality (Fig. 4). The latter showed that an identifiability problem occurred: a change in K_la can be compensated completely by a change in $K_{aff,g}$ (Vanrolleghem et al., 1995). Implementing different K_la values, however, did not influence the estimated v_{max} value, which confirms the absence of mass transfer limitation in the initial linear range of the recorded progress curve.

Multiresponse Fitting—Fitting Model I

In the sequel, it will be shown that an unequivocal (K_la, $K_{aff,g}$) combination can be identified using a new multiresponse fitting method. A multiresponse fitting method generally combines the results of different experiments (Johnson and Berthouex, 1975), in this case the three progress curves PC1, PC2, and PC3. The identification is based on the fact that each progress curve, due to the different biomass in each batch vessel, contains different information with respect to the gas:liquid mass transfer process. A different relationship between the implemented K_la and estimated $K_{aff,g}$ will be obtained for each progress curve, but these different relationships will show an intersection point corresponding to the true (K_la, $K_{aff,g}$) combination.

A graphical illustration of this multiresponse technique is presented in Figure 5, where the relationship between the implemented K_la value and the $K_{aff,g}$ estimate is shown for each recorded progress curve. The results show that, due to experimental error, not one but three intersection points are obtained in a relatively narrow range of K_la and $K_{aff,g}$: 172 h^{-1}, 57.7 ppm; 185 h^{-1}, 62.1 ppm; and 201 h^{-1}, 65.5 ppm. The estimated v_{max} values for the three progress curves PC1, PC2, and PC3 corresponded to 9.9, 10.1, and 10.5 nmol C_2H_4 mg^{-1} CDW min^{-1}, and can thus be considered identical to the values obtained by fitting model II (Table

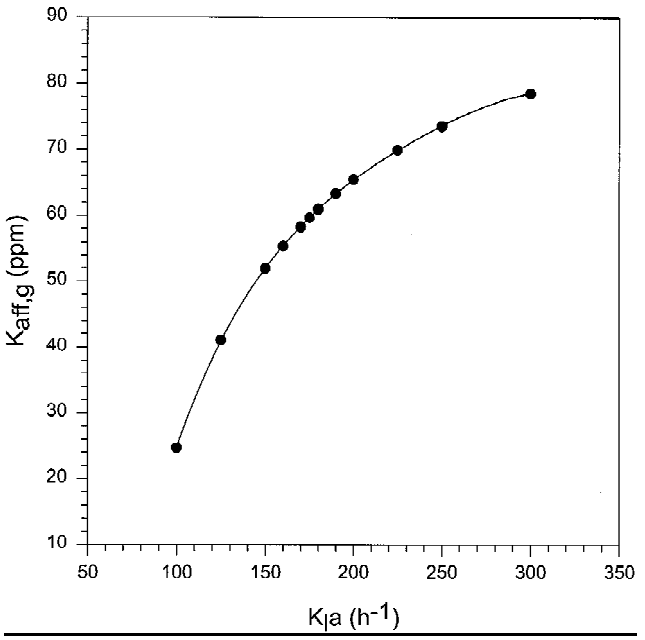

Figure 4. Estimated $K_{aff,g}$ values (●) when fitting model I to progress curve PC1 for different fixed values of K_la. The estimated v_{max} value and the value of the objective function corresponded, in each case, to 9.9 nmol · mg^{-1} CDW · min^{-1} and 4.16e-03, respectively. The obtained (K_la, $K_{aff,g}$) datapoints were smoothed (—) using a fourth-order polynomial (correlation >0.9999).

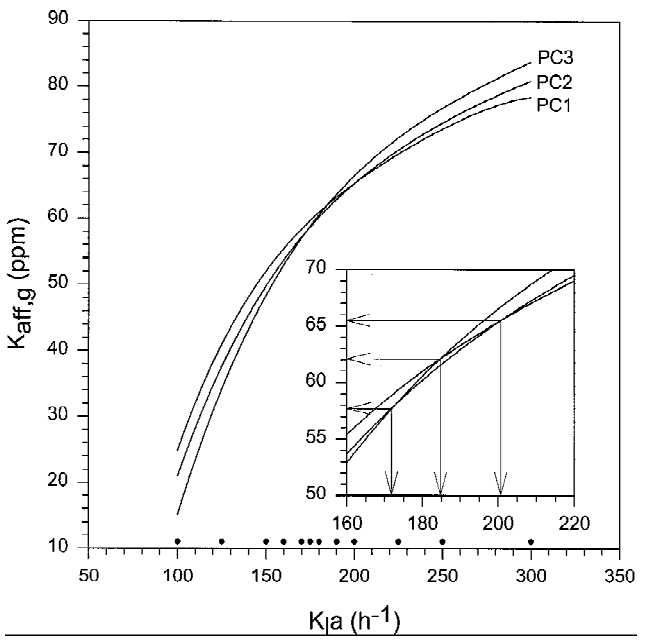

Figure 5. The three (K_la, $K_{aff,g}$) relationships obtained when fitting model I to the progress curves PC1, PC2, and PC3 separately, with implementation of the Blackman biokinetic function for different fixed values of K_la (●). Each relationship was smoothed using a fourth-order polynomial (correlation >0.9999). The inset enlarges the zone of intersection.

III). The mean value of the three estimates for each considered parameter corresponds to v_{max} 10.2 nmol C_2H_4 mg^{-1} CDW min^{-1}, $K_{aff,g}$ 61.8 ppm, and K_la 186 h^{-1}.

A direct multiresponse fitting procedure was also implemented in the computer fitting program. The direct multiresponse fitting resulted in a single K_la and $K_{aff,g}$ value estimated for the three progress curves. The v_{max} estimate, on the other hand, was allowed to depend on the progress curves. The parameter estimates obtained with the direct multiresponse fitting (Table IV) are comparable with the estimates obtained with the graphical multiresponse fitting, which illustrates that the latter can be used as a less software-demanding alternative. The direct multiresponse fitting confirmed that, in the case of model I also, the Blackman biokinetic function resulted in a better quality of fit (Table IV).

The $K_{aff,g}$ estimate obtained by fitting model I (Table IV) shows that the fitting of model II resulted in an overestimation of $K_{aff,g}$ by at least a factor 1.7 (Table III). The K_la estimate obtained by fitting model I (185 h^{-1}) (Table IV) can certainly be regarded as a realistic value in comparison with the value required to justify parameter estimation by fitting model II (2000 h^{-1}) (Appendix). Comparison of the estimated Blackman biokinetic parameters, v_{max} and $K_{aff,g}$, with the values given by van Ginkel et al. (1986), for the biodegradation of ethene by resting cell suspensions of *Mycobacterium* E3, namely v_{max} 50 nmol mg^{-1} protein min^{-1} and $K_{aff,g}$ 100 ppm, is not straightforward. First, van Ginkel et al. (1986), characterized the strain using a Monod biokinetic function and, second, no procedure to account for possible mass transfer limitation was reported in their work.

Influence of H—Fitting Model I

The parameter, *H*, is assumed to be known and fixed at a certain value during model fitting. Normally, it is fixed at the reference value of the air:water system at the temperature of the experiment. However, electrolytes as well as organic substances in aqueous solution usually decrease the solubility of gases as compared with pure water (Dewulf et al., 1995; Schumpe et al., 1982; Yurteri et al., 1987).

The possible influence of *H* on the fitting results for model I is illustrated in Table V for the case of progress curve PC3. The results show that a hypothetical decrease of *H* by 10% had no influence on the estimated values of v_{max}. However, the decrease of *H* resulted in an increase of the estimated $K_{aff,g}$ and $K_{aff,l}$ values of 9.2% and 21.4%, respectively (Table V). A smaller *H* value corresponds to an increased solubility [Eq. (3)], which implies that the C_g values of a recorded progress curve will correspond to higher C_l values in the calculation of model I during the model fitting. Model I interprets the latter mathematically as an increased $K_{aff,l}$ value. The increase of the $K_{aff,l}$ estimate is partially compensated for when the corresponding $K_{aff,g}$ value is calculated using Eq. (6). The real biological affinity parameter, however, is $K_{aff,l}$ and not $K_{aff,g}$, because biodegradation takes place in the liquid phase.

A possible explanation for the independence of the estimated v_{max} value on the implemented *H* value is that the initial linear course of the compound gas concentration in the progress curve corresponds with an identical linear course (i.e., identical slope) of the compound concentration in the liquid phase.

The dependency of the affinity coefficient on *H* introduces an additional uncertainty in the model fitting, which has not been considered in previous studies (de Bont, 1976; Robinson and Tiedje, 1982). In principle, the *H* value should therefore be determined experimentally for the air:resting cell suspension system.

Table IV. Results of fitting model I to the progress curves PC1, PC2, and PC3 using direct multiresponse fitting with implementation of the Blackman, Teissier, and Monod biokinetic functions.

Biokinetic function	v_{max} estimate[a]	$K_{aff,g}$ estimate	K_la estimate	Minimized SSR_{rel}
Blackman	10.2	61.9	185	1.03e-02
Teissier	10.4	36.9	120	2.60e-02
Monod	12.3	91.1	167	1.49e-01

[a]The v_{max} estimate is the mean value of the estimates for the three respective progress curves.

Table V. Fitting model I[a] with implementation of the Blackman biokinetic function to progress curve PC3 assuming a decrease of *H* with 10% in comparison with the air:water reference value.

	H assumed	v_{max} estimate	$K_{aff,g}$ estimate	$K_{aff,l}$ estimate
Reference value	8.3	10.53	60.51	8.36
10% decreased	7.5	10.54	66.06	10.15

[a]K_la was fixed at 180 h^{-1}.

CONCLUSIONS

Fitting model II to the recorded progress curves, which did not incorporate mass transfer aspects, resulted in a large overestimation of $K_{aff,g}$, because the progress curves were mass transfer limited. The progress curves were only mass transfer limited in the nonlinear range so that acceptable v_{max} estimates still could be obtained. It is very important to note that the mass transfer limitation did not block the ability to obtain a good fit of model II, because the modeling error was lumped in the estimated affinity coefficient. The latter implies a risk of overlooking the problem.

A new multiresponse method was developed, allowing to obtain more reliable estimates of $K_{aff,g}$ and also K_la from a restricted number of mass transfer limited progress curves by fitting model I, which incorporated both mass transfer and biodegradation aspects. The essence is that the different biomass concentrations applied result in different mass transfer limitation conditions so that the identifiability of the parameters is guaranteed. In principle, the approach requires

that the dimensionless gas:liquid partition coefficient, H, is determined experimentally.

For fitting both model I and model II, the Blackman biokinetic function allowed a superior fit of the recorded progress curves in comparison with the more traditionally used Monod biokinetic function. This illustrates the importance of evaluating an alternative biokinetic function.

The new method proposed in this article can, through a better characterization of the biodegradation process, help to evaluate the feasibility of bioremediation processes, which are determined by parameters such as the maximum specific degradation rate and the affinity coefficient and in which mass transfer limitation can interfere. More specifically, the proposed method can be an important tool in evaluating the feasibility of biological waste gas treatment, especially when low water soluble gaseous pollutants are directly involved.

APPENDIX

Evaluation of Required Overall Ethene Volumetric Mass Transfer Coefficient

The relatively small liquid volume in the batch vessel and the vessel's geometry did not allow experimental determination of the overall volumetric mass transfer, $K_l a$, neither for ethene nor oxygen. To assess the feasibility of the required $K_l a$ value for ethene (minimum 2000 h^{-1}), it was related to the corresponding $K_l a$ value for oxygen for which literature data are available for shaken flasks.

According to the two resistance theories, $K_l a$ is defined as (Treybal, 1980):

$$\frac{1}{K_l a} = \frac{1}{K_l} \cdot \frac{1}{a} = \left(\frac{1}{H \cdot k_g} + \frac{1}{k_l} \right) \cdot \frac{1}{a} \qquad \text{(A1)}$$

Low water soluble compounds, such as ethene, can be considered to exhibit complete liquid phase mass transfer behavior, so it can be assumed that:

$$H \cdot k_g >> k_l \qquad \text{(A2)}$$

and that Eq. (A1) becomes:

$$K_l a = k_l \cdot a \qquad \text{(A3)}$$

If the liquid interphase is in turbulent motion, as can be expected under conditions of intense agitation, it can be assumed that (van Suijdam et al., 1978):

$$kl \propto \sqrt{D_l} \qquad \text{(A4)}$$

Combining Eqs. (A3) and (A4) gives:

$$(K_l a)_{O_2} = \sqrt{\frac{D_{l,O_2}}{D_{l,C_2H_4}}} (K_l a)_{C_2H_4} \qquad \text{(A5)}$$

The diffusion coefficient for ethene in water at 25°C was set equal to 1.54e-5 $cm^2\ s^{-1}$. This value is the mean taken from the literature (Huq and Wood, 1968) The diffusion coefficient for oxygen in water at 25°C was set equal to 2.5e-5 $cm^2\ s^{-1}$ (Perry and Chilton, 1974). Substitution of these two values in Eq. (A5) indicates that the $K_l a$ value for oxygen should be a factor 1.27 higher than the corresponding $K_l a$ value for ethene. A $K_l a$ value of 2000 h^{-1} would, therefore, correspond to a $K_l a$ value for oxygen of about 2540 h^{-1}. This value is hardly attainable under conditions of batch shakers. The maximum $K_l a$ value for oxygen, determined by van Suijdam et al. (1978), under extreme shaking conditions, corresponded to 428 h^{-1}.

NOMENCLATURE

a	gas:liquid interface surface per unit volume liquid (m^{-1})
CDW	cell dry weight
C_g	gas concentration (ppm)
C_l	liquid concentration ($\mu g\ L^{-1}$)
C_l^*	equilibrium compound liquid concentration for C_g ($\mu g\ L^{-1}$)
D_l	diffusion coefficient in the liquid phase ($cm^2\ s^{-1}$)
H	dimensionless gas:liquid distribution coefficient on a volumetric basis (−)
$K_{aff,g}$	affinity parameter in gas concentration units (ppm)
$K_{aff,l}$	affinity parameter in liquid concentration units ($\mu g\ L^{-1}$)
k_g	mass transfer coefficient for the gas interphase ($m\ h^{-1}$)
k_l	mass transfer coefficient for the liquid interphase ($m\ h^{-1}$)
K_l	overall gas:liquid mass transfer coefficient ($m\ h^{-1}$)
$K_l a$	volumetric overall gas:liquid mass transfer coefficient (h^{-1})
n	number of fitted datapoints (−)
SSR_{rel}	sum of squared relative residuals (−)
t	time (min)
v	specific degradation rate (nmol C_2H_4 mg^{-1} CDW min^{-1})
V_g	volume of the gaseous phase (mL)
V_l	volume of the liquid phase (mL)
v_{max}	maximum specific degradation rate (nmol C_2H_4 mg^{-1} CDW min^{-1})
X	biomass concentration (mg CDW mL^{-1})

Note: Listed units are only intended for presentation of the results and not for direct substitution in the biophysical model equations which require SI units.

References

l'Air Liquide. 1976. Encyclopedie des gaz. Elsevier, Amsterdam.

de Bont, J. A. M. 1976. Oxidation of ethene by soil bacteria. Antonie van Leeuwenhoek **42**: 59–71.

Brent, R. P. 1973. Algorithms for minimization without derivatives. Prentice Hall, Englewood Cliffs, NJ.

Dewulf J., Drijvers D., Van Langenhove, H. 1995. Measurement of Henry's law constant as function of temperature and salinity for the low temperature range. Atmos. Environ. **29**: 323–331.

van Ginkel, C. G., de Bont, J. A. M. 1986. Isolation and characterisation of alkene-utilizing *Xanthobacter* spp. Arch. Microbiol. **145**: 403–407.

van Ginkel, C. G., Welten, H. G. J., de Bont J. A. M., Boerrigter, H. A. M. 1986. Removal of ethene to very low concentrations by immobilised Mycobacterium E3. J. Chem. Technol. Biotechnol. **46**: 593–598.

Habets-Crützen, A. Q. H., Brink, L. E. S., van Ginkel, C. G., de Bont, J. A. M., Tramper, J. 1984. Production of epoxides from gaseous alkenes by resting-cell suspensions and immobilized cells of alkene-utilizing bacteria. Appl. Microbiol. Biotechnol. **20**: 245–250.

Huq, A., Wood, T. 1968. Diffusion coefficient of ethylene gas in water. J. Chem. Eng. Data **13**: 256–259.

Johnson, D. B., Berthouex, P. M. 1975. Using multiresponse data to estimate biokinetic parameters. Biotechnol. Bioeng. **17**: 571–583.

Miller, J. N. 1991. Basic statistical methods for analytical chemistry. Part 2. Calibration and regression methods-a review. Analyst **116**: 3–14.

Moser, A. 1985. Kinetics of batch fermentations. In: H.-J. Rehm and G. Reed (eds.), Biotechnology, vol. 2. Fundamentals of biochemical engineering. VCH, Weinheim.

Perry, R. H., Chilton, C. H. 1974. Chemical engineer's handbook. McGraw-Hill, London.

Powel, E. O. 1967. The growth rate microorganisms as a function of substrate concentration. In: E. O. Powell, C. G. T. Evans, R. E. Strange, and D. W. Tempest (eds.), Microbial physiology and continuous culture. HMSO, London.

Robinson, J. A. 1985. Determining microbial kinetic parameters using nonlinear regression analysis. Advantages and limitations in microbial ecology. Adv. Microb. Ecol. **8**: 61–114.

Robinson, J. A., Tiedje, J. M. 1982. Kinetics of hydrogen consumption by rumen fluid, anaerobic digestor sludge, and sediment. Appl. Environ. Microbiol. **44**: 1374–1384.

Robinson, J. A., Tiedje, J. M. 1983. Nonlinear estimation of Monod growth kinetic parameters from a single substrate depletion curve. Appl. Environ. Microbiol. **45**: 1453–1458.

Saéz, P. B., Rittmann, B. E. 1992. Model-parameter estimation using least squares. Water Res. **26**: 789–796.

Schumpe, A., Quicker, G., Deckwer, W.-D. 1982. Gas solubilities in microbial culture media. In: A. Fiechter (ed.), Advances in biochemical engineering, vol. 24, Reaction engineering. Springer, Berlin.

Söderström, T., Stoïca, P. 1989. Model validation and model structure determination. In: System identification. Prentice Hall, New York.

van Suijdam, J. C., Kossen, N. F. W., Joha, A. C. 1978. Model for oxygen transfer in a shake flask. Biotechnol. Bioeng. **20**: 1695–1709.

Treybal, R. E. 1980. Mass transfer operations. McGraw-Hill, New York.

Vanrolleghem, P., Verstraete, W. 1993. Simultaneous biokinetic characterisation of heterotrophic and nitrifying populations of activated sludge with an on-line respirographic biosensor: Water Sci. Technol. **28**: 377–387.

Vanrolleghem, P., Van Daele, M., Dochain, D. 1995. Practical identifiability of a biokinetic model of activated sludge respiration. Water Res. **29**: 2561–2570.

Yurteri, C., Ryan, D. F., Callow, J. J., Gurol, M. D. 1987. The effect of chemical composition of water on Henry's law constant. J. Water Pollut. Control Fed. **59**: 950–956.